J Musculoskelet Neuronal Interact 2010; 10(2):180-187

Original Article

Hylonome

Skeletal phenotype of mice with a null mutation in Cav 1.3 L-type calcium channel

J. Li[1], L. Zhao[2], I.K. Ferries[1], L. Jiang[1], M.Z. Desta[1], X. Yu[1], Z. Yang[3], R.L. Duncan[4], C.H. Turner[2]

[1]Department of Biology, Indiana University Purdue University Indianapolis, USA; [2]Department of Orthopedic Surgery, Indiana University School of Medicine, USA;[3]Department of Pediatrics, Herman B Wells Center for Pediatric Research, Indiana University School of Medicine; [4]Department of Biological Sciences, University of Delaware, USA

Abstract

This study aimed to understand the role of Cav1.3, one of the four L-type voltage sensitive calcium channels (VSCC) α_1 subunits, in the skeletal response to mechanical loading and intermittent PTH treatment. The Cav1.3 mRNA is expressed in osteoblasts. The Cav1.3 mRNA level in male wild type mice is higher than those in female. Loss of Cav1.3 resulted in a smaller skeleton in male mice as indicated by significantly lower body weight, less bone mineral content and smaller cross-sectional area of femoral midshaft. However, the osteogenic response to mechanical loading of the ulna was normal in Cav1.3$^{-/-}$ compared to the normal control mice. Male mice Cav1.3$^{-/-}$ were then treated daily with PTH at a dose of 40 μg/kg. A 6-week course of intermittent PTH treatment enhanced bone mineral content and mechanical strength equally in wild type control and Cav1.3 null mice. We also found that Cav1.2 subunit significantly increases in the absence of Cav1.3 gene. In conclusion, Cav1.3 is involved in bone metabolism, especially in male mice. Cav1.3 does not mediate osteoblast response to mechanical loading and PTH. Our data suggest that Cav1.1 and Cav1.2 subunits may substitute for Cav1.3 to maintain bone response to mechanical loading.

Keywords: Mechanotransduction, Osteogenesis, Voltage Sensitive Calcium Channel, Parathyroid Hormone, Bone Density

Introduction

There are many means by which bone formation can be stimulated to strengthen the skeleton. Mechanical loading and intermittently dosed parathyroid hormone (PTH) are two of the most potent anabolic stimuli for bone. Various biochemical pathways in osteoblasts are activated by these stimuli, including pathways associated with intracellular Ca^{2+} concentration ($[Ca^{2+}]_i$), resulting from both extracellular Ca^{2+} entry and release of Ca^{2+} from intracellular stores[1,2]. We have demonstrated that extracellular Ca^{2+} entry via L-type voltage sensitive Ca^{2+} channels (VSCC) is important in osteoblast proliferation, *in vitro*, and mechanically-induced bone formation *in vivo*[3,4]. In addition, PTH treatment has been shown to modulate L-type VSCC activity in osteoblasts and inhibition of his channel significantly reduces Ca^{2+} signaling induced by PTH[2,5]. Furthermore, PTH and mechanical loading may act synergistically on bone formation[6,7]. Our previous studies show that verapamil, an L-type VSCC blocker, suppresses bone formation in animals subjected to the combination of intermittent PTH plus loading. These data suggest that PTH enhances load-induced bone formation through involvement of L-type VSCC[7] and we hypothesize that L-type VSCCs play an important role in mediating load- and PTH-induced bone formation.

L-type VSCC, a ubiquitously expressed subfamily of voltage sensitive Ca^{2+} channels, are heteromeric protein complexes characterized by their sensitivity to dihydropyridines[8]. The α_1 subunit forms the pore of the channel and contains the sequences for the dihydropyridine receptor and the voltage sensor. Four different genes code for the L-type VSCC α_1 subunit, suggesting that each may provide a unique function in different cell types[9]. These have been designated Cav1.1, Cav1.2, Cav1.3 and Cav1.4. Three of those L-type VSCC isoforms, Cav1.1, Cav1.2 and Cav1.3, have been found in osteoblastic cells[10]. However, it is not clear which α_1 subunit mediates the anabolic effect of loading and PTH. Recent work shows that

The authors have no conflict of interest.

Corresponding author: Jiliang Li, Ph.D., Department of Biology, Indiana University Purdue University Indianapolis, 723 West Michigan Street, SL 306, Indianapolis, IN 46202, USA
E-mail: jilili@iupui.edu

Edited by: J. Gasser
Accepted 1 March 2010

Cav1.2 is the primary site for Ca^{2+} influx into osteoblast after stimulation with 1,25 Vitamin D[11], suggesting that Cav1.2 is important in osteoblast activation. Much less is known about the role of Cav1.3 in osteoblast activity and bone formation. PTH has been shown to activate Cav1.3 in osteoblastic cells[10]. Genetic ablation of Cav1.3 subunit results in congenital deafness and dysfunction of pancreatic β cells and cardiac sinoatrial node[12-14]. One previous study elucidates the role played by Cav1.3 neuronal L-type Ca^{2+} channels in phosphorylated cAMP response element-binding protein (pCREB) signaling[15]. PTH can activate CREB expression in osteoblasts[16]. Therefore, we hypothesized a role for Cav1.3 in bone biology. Since L-type VSCCs appear to mediate mechanical loading and PTH signaling in osteoblasts, we tested the hypothesis that Cav1.3 was necessary for bone anabolism following these stimuli.

Materials and Methods

Experimental animals

Cav1.3 knock-out (Cav1.3 $^{-/-}$) mice were obtained from D. James Surmeier (Feinberg School of Medicine, Northwestern University, Chicago, U.S.A.), who originally received the animals from Joerg Striessnig (Institut Fur Biochemische Pharmakologie, Innsbruck, Austria)[13]. The mice were rederived and backcrossed on a C57Bl/6 background in the Northwestern University barrier facility. We interbred the heterozygous mice with the null mutation of Cav1.3 (Cav1.3$^{+/-}$) and obtained wild-type (Cav1.3$^{+/+}$), heterozygous (Cav1.3$^{+/-}$) and homozygous mutant (Cav1.3 $^{-/-}$) offspring in the expected Mendelian genetic frequencies. All procedures performed in this study were in accordance with the Indiana University Animal Care and Use Committee Guidelines.

In vivo Ulna Loading

Mechanical loading of the skeleton was carried out using the ulna loading protocol described by Torrance et al[17]. Sixteen male and sixteen female Cav1.3$^{+/+}$ and Cav1.3 $^{-/-}$ mice (18 weeks old) were anesthetized with veterinary isoflurance and subjected to loading of the right forearms for two minutes (120 cycles) at a peak force of 2.5 Newton using a 2-Hz haversine waveform. Loading was applied on three consecutive days using an electromagnetic actuator (Bose ElectroForce 3200 series; EnduraTEC, Minnetonka, MN, USA). The left forearms were not loaded and served as internal controls for loading effects. All mice were allowed normal cage activity between loading sessions and afterward. Intraperitoneal injections of calcein (30 mg/kg body weight; Sigma) and alizarin (50 mg/kg body weight; Sigma) were administered 5 and 11 days after the first loading day. All animals were sacrificed 14 days after the first loading day.

Right (loaded) and left (control) ulnas were processed for histomorphometry to evaluate load-induced bone formation. Femurs were used to investigate the bone size and bone mineral density of male and female Cav1.3$^{-/-}$ mice in comparison with wild-type Cav1.3$^{+/+}$ mice. All the left femurs were scanned for BMD using pixiMUS and then tested for biomechanical properties using a materials testing machine. The cross sections of all the right femurs were sectioned and used for measurement of bone geometry and formation.

In Vivo PTH Treatment

Twenty-nine male Cav1.3$^{+/+}$ and Cav1.3 $^{-/-}$ mice were administered subcutaneous injections of human PTH-(1-34) (40 μg/kg) or vehicle (99.7% normal saline, 0.2% bovine serum albumin and 0.1% HCl) daily for 6 weeks. Intraperitoneal injections of calcein (30 mg/kg body weight; Sigma) and alizarin (50 mg/kg body weight; Sigma) were administered 9 and 3 days before sacrifice. After mice were sacrificed, the left femurs were collected for pixiMUS densitometer and mechanical testing. The right femurs were processed for histological measurement.

RNA Isolation from Calvarial Osteoblasts and Bone Tissues

Calvarial osteoblasts were obtained from 3-5 day-old neonatal calvariae from Cav1.3 WT and KO mice. Calvariae from the same genotype were grouped and subjected to five sequential 15-min digestions with an enzyme mixture of 1.5 units/ml collagenase (Roche Molecular Biochemicals, Penzberg) in PBS and 0.05% trypsin/ 1mM EDTA (Gibco) at 37°C on a rocking platform. The first digest was discarded and the second to the fifth digests were passed through a 40-mm cell strainer (Falcon, BD Biosciences) and pooled. Cells were collected after centrifugation at 2,500 × g for 8 min and plated in α-modified essential medium with 10% fetal bovine serum, 100 units/ml of penicillin, and 100 μg/ml of streptomycin in a T25 culture flask (Costar; Corning, Corning, NY) and grown to confluence. After reaching confluence, cells were collected in TRIzol reagent (Invitrogen, CA) and stored at -80°C for total RNA isolation.

Total RNA was also isolated from the femurs of 6 - 8 weeks old Cav1.3 KO and WT mice. After sacrifice, both limbs of the newborn mice and adult femurs will be dissected out immediately, snap frozen in liquid nitrogen and stored at -80°C until RNA isolation.

Reverse Transcription and real-time PCR

Total RNA was isolated using TRIzol reagent (Invitrogen, CA). Using 1 μg of total RNA isolated from both calvarial osteoblasts and femurs, reverse transcription was conducted with the first strand cDNA synthesis kits (GE Healthcare). Regular PCR was performed to confirm the Cav1.3 expression in primary osteoblasts and femurs using Platinum PCR Supermix (Invitrogen, CA) with primers (Forward: GCAAACTATGCAAGAGGCACC and Reverse: GGGAGAGAGATCCTACAGGTGG). Quantitative real-time PCR was performed using ABI 7500 with Taqman PCR master mix kits (Applied Biosystems). We evaluated the mRNA levels of Cav1.1 (Assay ID no. Mm00489257_m1), Cav1.2 (Assay ID no. Mm00437923_mH) and Cav1.3 expression (Mm01209919_m1) using TaqMan gene expression assays (Applied Biosystems, CA). GAPDH (Assay

ID no. Mm03302249_g1) was used for internal control. There was no difference in GAPDH mRNA levels between Cav1.3$^{+/+}$ and Cav1.3$^{-/-}$ mice. The relative mRNA abundance for the Cav1.1, Cav1.2 and Cav1.3 mRNA with respect to the level of GAPDH mRNA was used.

Peripheral Dual-Energy X-ray Absorptionmetry (pixiMUS)

To study bone phenotype, bone mineral content (BMC) and bone mineral density (BMD) of the left femurs that were collected from the loading study were evaluated *in vitro* using peripheral dual-energy x-ray absorptiometry (pDXA; PIXIMus II; GE-Lunar Corp., Madison, WI).

In the PTH study, Bone mineral content (BMC) of the whole body was evaluated using the pixiMUS. Mice were anesthetized via inhalation of 2.5% isoflurane (IsoFlo; Abbott Laboratories, North Chicago, IL) mixed with O2 (1.5 liter/min) for a total ~7-8 min during both induction and scanning. The mice were placed in prone position on a specimen tray and scanned. The head was excluded from the total body scans. Scans were performed right before PTH treatment and at the end of experiment.

Biomechanical Testing

Femurs were brought to room temperature slowly (~2 h) in a saline bath and tested at the mid-diaphysis by three-point bending using a microforce materials testing machine (Vitrodyne V1000; Liveco, Inc., Burlington, VT). Load was applied in the anteroposterior direction midway between two supports positioned 10 mm apart. Tests were conducted at a cross-head speed of 0.2 mm/s, during which force-displacement curves were generated, from which ultimate force (F_U; N), stiffness ((S; N/mm) and work to failure (U; mJ) were calculated. F_U represents the strength of the bone, whereas U is a measure of the energy required to break the bone.

Histomorphometry

Bone specimens were immersed in 10% neutral buffered formalin for 48 h to fix the tissues. The specimens were then dehydrated in graded alcohols, cleared in xylene, and embedded in methyl methacrylate. Using a diamond-embedded wire saw (Histo-saw; Delaware Diamond Knives, Wilmington, DE, U.S.A) Transverse thick sections (70 μm) were cut at the ulnar and femur midshafts, and further ground to a final thickness of 20 μm and then mounted unstained on microscope slides. One section per limb was read on a Nikon Optiphot flurescence microscope (Nikon, Inc., Garden City, NJ) using the Bioquant digitizing system (R&M Biometrics, Nashville, TN). The following primary data were collected from the periosteal surface at x250 magnification: total perimeter (B.Pm); single label perimeter (sL.Pm); double label perimeter (dL.Pm), and double label area (dL.Ar). From these primary data, the following derived quantities were calculated: mineralizing surface (MS/BS=[1/2sL.Pm+dL.Pm]/B.Pm ×100; %); mineral apposition rate (MAR = dL.Ar/dL.Pm/6 days; μm/day) and bone formation rate (BFR/BS = MAR × MS/BS × 3.65; $\mu m^3/\mu m^2$ per year). For the loading study, a new set of relative (r) values: rMS/BS, rMAR, and rBFR/BS using the left ulna (nonloaded) values subtracted from the right ulna (loaded) values showed purely mechanically induced bone formation.

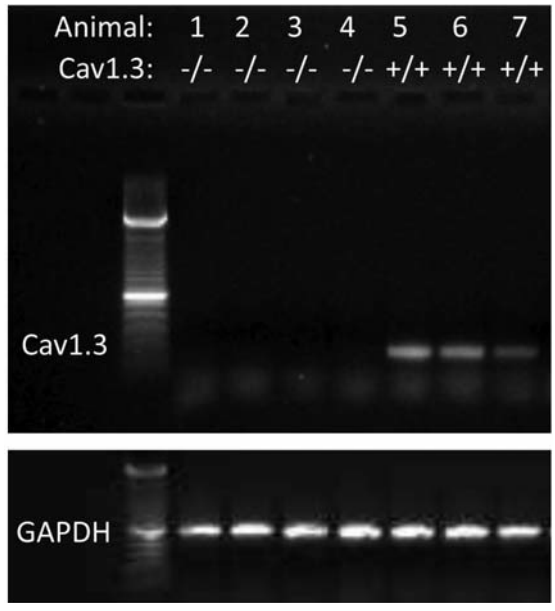

Figure 1. Loss of Cav1.3 expression was confirmed in Cav1.3$^{-/-}$ mice by RT-PCR from RNA extracted from homogenized femurs of 6-8 weeks old mice. Four Cav1.3$^{-/-}$ mice (mice 1, 2, 3 and 4) and three Cav1.3$^{+/+}$ mice (mice 5, 6 and 7) were used for expression confirmation. The 180-bp PCR product was evident in Cav1.3$^{+/+}$ but not Cav1.3$^{-/-}$ mice.

For the sections from distal femurs, the 5μm thick frontal sections were cut using a microtome (Leica, Germany) and mounted unstained on microscope slides. The following primary data were collected from the metaphyseal area, 0.5 mm below the growth plate and 0.5 mm away from the intracortical surface, at ×250 magnification: tissue area (T.Ar), trabecular bone area (tB.Ar), trabecular bone perimeter (tB.Pm), single label perimeter (sL.Pm), double label perimeter (dL.Pm), and double label area (dL.Ar). From these primary data, the following derived quantities were calculated: bone volume (BV/TV = tB.Ar/T.Ar × 100; %), mineralizing surface (MS/BS = [1/2sL.Pm+dL.Pm]/B.Pm ×100; %); mineral apposition rate (MAR = dL.Ar/dL.Pm/6 days; μm/day) and bone formation rate (BFR/BS = MAR × MS/BS × 3.65; $\mu m^3/\mu m^2$ per year).

Statistical analysis

The data are expressed as mean ± SEM (standard error of the mean). Differences between the loaded (right) and nonloaded (left) limbs were tested using paired t-tests. Differences among group means were tested for significance by analysis of variance (ANOVA), followed by Fisher's protected least significant difference (PLSD) for all the pairwise comparisons. PTH effect comparisons were performed using a two-way analysis of variance with sex and genotype as independent variables. Statistical significance was assumed for $p<0.05$.

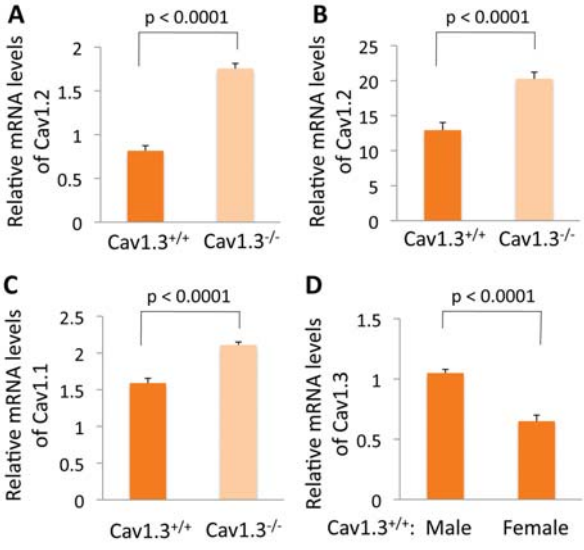

Figure 2. Real-time PCR analysis of the expression of Cav1.1, Cav1.2 and Cav1.3 normalized by GAPDH in Cav1.3 null mice and the normal control. Relative Cav1.2 expression was quantified by Real time RT- PCR from RNA extracted from primary calvarial osteoblasts isolated from four Cav1.3$^{+/+}$ and four Cav1.3$^{-/-}$ mice (**A**) and homogenized femurs of 6-8 weeks old mice, four male Cav1.3$^{+/+}$ and three male Cav1.3$^{-/-}$ mice (**B**). Relative mRNA levels of Cav1.1 in femurs of four male Cav1.3$^{+/+}$ and three male Cav1.3$^{-/-}$ mice (**C**). Relative mRNA levels of Cav1.3 in three male and three female wild type mice (**D**).

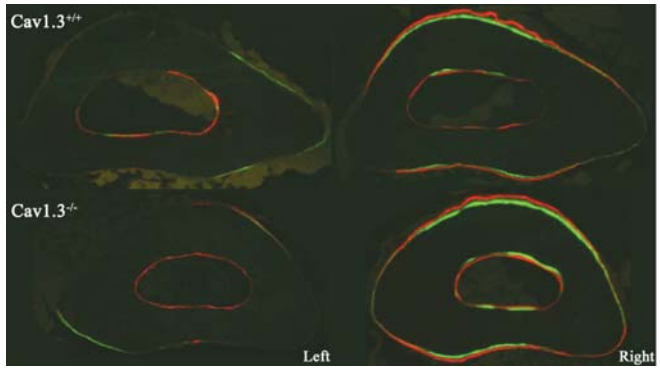

Figure 3. Mice with Cav1.3 null mutation have normal osteogenic response to mechanical loading. Axial compression was applied to mice ulnae to produce mechanically induced new bone formation. The figure shows midshaft ulnar tissue sections from control (left) and loaded (right) forearms among male wild type and Cav1.3 null mice given fluorochrome injections after loading show a robust bone formation response on the medial (top) and lateral (bottom) surfaces of both the loaded wild type and Cav1.3 null mice.

Results

Gene expression in Calvarial Osteoblasts and Femurs

Cav1.3 mRNA expression was identified in normal calvarial osteoblasts and femurs. Loss of Cav1.3 expression was confirmed in Cav1.3$^{-/-}$ mice by RT-PCR from RNA extracted from primary osteoblasts and homogenized femurs (Figure 1).

The Cav1.2 mRNA in primary osteoblasts and femurs as well as **Cav1.1 mRNA** in femurs were found in both Cav1.3$^{+/+}$ and Cav1.3$^{-/-}$ mice. However, **Cav1.1** and Cav1.2 mRNA levels in Cav1.3$^{-/-}$ mice were significantly higher (33% and 67%, respectively, $p<0.0001$) than that in Cav1.3$^{+/+}$ mice (Figure 2). In wild type mice, expression of Cav1.3 mRNA in male mice was about 38% higher ($p<0.0001$) than female mice.

Sex dependent deficiency in bone mass and geometry in Cav1.3-null mice

The average body weight was slightly different between female Cav1.3$^{-/-}$ and Cav1.3$^{+/+}$ mice, but male Cav1.3$^{-/-}$ mice have significantly lower body weight than male WT mice ($p<0.01$; Table 1). Femoral lengths were similar among all the animals. However, male Cav1.3$^{-/-}$ mice exhibit smaller cross-sectional area at midshaft femur in comparison with male WT mice ($p<0.01$; Table 1). Both femoral bone mineral density (BMD) and bone mineral content (BMC) are significantly lower in male Cav1.3$^{-/-}$ mice than WT ($p<0.01$; Table 1). There was no difference in BMD and BMC between female Cav1.3$^{-/-}$ and WT mice.

Histomorphometry at the femoral midshaft indicated that bone formation at periosteal surface is similar among all the animals. But the mineral appositional rate was significantly higher in male Cav1.3$^{+/+}$ mice than the other groups ($p<0.05$).

Osteogenic response to mechanical loading in vivo

To directly investigate the role of Cav1.3 in bone mechanoresponsiveness *in vivo*, we subjected Cav1.3$^{-/-}$ and Cav1.3$^{+/+}$ mice to *in vivo* mechanical loading and measured the bone formation response histomorphometrically. Cross-sections of loaded ulnas from both Cav1.3$^{+/+}$ and Cav1.3$^{-/-}$ revealed new periosteal and endocortical lamellar bone formation, mostly on the medial and lateral quadrants (Figure 3). Histomorphometric measurements indicate the relative periosteal bone formation rate (BFR/BS in the loaded ulna minus BFR/BS in the nonloaded ulna) was not significantly different in Cav1.3$^{-/-}$ mice compared with WT mice (Table 2). These data indicate that loss of Cav1.3 does not affect load-induced bone formation.

Parathyroid Hormones is equally anabolic in Cav1.3$^{-/-}$ and Cav1.3$^{+/+}$ mice

We treated 14-15 weeks old male mice for 6 weeks with daily injections of PTH-(1-34) (40 μg/kg) or vehicle, and monitored whole bone mass changes by baseline and final pixiMUS scans. Percent change in bone mineral content (baseline BMC versus final BMC) showed in Figure 2. Without PTH treatment BMC decreased by 8.7% in WT and 9.7% in Cav1.3$^{-/-}$ mice. However, PTH treatment improved whole body BMC by 5.6% in WT and 7% in Cav1.3$^{-/-}$ mice. The similar changes in BMD were found in WT and Cav1.3$^{-/-}$ mice following PTH treatment (Figure 4). Analysis of variance revealed significant overall

Parameter	Male		Female	
	Cav1.3 +/+	**Cav1.3$^{-/-}$**	**Cav1.3$^{+/+}$**	**Cav1.3$^{-/-}$**
Animal number	n=8	n=8	n=8	n=8
Body mass (g)	28.14±0.68[a]	25.05±0.57[a,b]	22.88±1.14[a]	20.93±1.19[a]
Femoral length (mm)	15.69±0.10	15.45±0.10	15.41±0.13	15.22±0.18
Midshaft femur geometric properties				
Cortical area (mm^2)	0.91±0.03[a]	0.77±0.03[b]	0.77±0.01[a]	0.74±0.04
Bone marrow area (mm^2)	1.23±0.07[a]	0.98±0.02[b]	0.91±0.03[a]	0.86±0.04
Midshaft femur histomorphometry				
Periosteal surface				
MS/BS (%)	37.70±2.17	33.89±2.40	35.43±3.58	30.30±1.65
MAR (μm/day)	1.00±0.10	0.96±0.09	0.87±0.13	0.99±0.09
BFR/BS (μm^3/μm^2/yr)	134.21±13.72	112.92±8.87	100.92±11.54	106.54±5.18
Endocortical Surface				
MS/BS (%)	44.14±1.81	43.25±1.49	38.89±2.73	40.67±2.39
MAR (μm/day)	1.67±0.36[c]	0.87±0.13[d]	0.91±0.10[c]	1.06±0.07
BFR/BS (μm^3/μm^2/yr)	253.66±45.64[a]	134.83±20.56[b]	123.63±11.95[a]	158.58±15.26
Femoral Bone Mineral				
BMD (mg/cm^2)	0.061±0.002	0.053±0.002[b]	0.057±0.001	0.053±0.002
BMC (mg)	0.06±0.003[b]	0.048±0.002[a]	0.049±0.002[b]	0.045±0.003

MS/BS: mineralizing surface.
MAR: mineral appositional rate.
BFR/BS: bone formation rate.
BMD: bone mineral density.
BMC: bone mineral content.
[a]p<0.01, significantly different between sexes for a given genotype.
[b]p<0.01, significantly different from the WT control.
[c]p<0.05, significantly different between sexes for a given genotype.
[d]p<0.05, significantly different from the WT control.

Table 1. Baseline skeletal phenotype in 20-week-old Cav1.3$^{+/+}$ and Cav1.3$^{-/-}$.

Parameters	Male					
	Cav1.3$^{+/+}$ (n=8)			**Cav1.3$^{-/-}$ (n=8)**		
	Right	**Left**	**Relative**	**Right**	**Left**	**Relative**
MS/BS (%)	39.30±5.69*	9.52±2.37	29.78±5.55	63.87±3.79*	20.72±4.59	43.16±3.58
MAR (μm/day)	1.12±0.13*	0.32±0.02	0.80±0.11	1.16±0.07*	0.52±0.11	0.64±0.14
BFR/BS (μm^3/μm^2/yr)	162.38±30.07*	11.70±3.59	150.68±28.68	275.56±23.60*	45.67±16.28	229.89±18.70
	Female					
	Cav1.3$^{+/+}$ (n=7)			**Cav1.3$^{-/-}$ (n=7)**		
	Right	**Left**	**Relative**	**Right**	**Left**	**Relative**
MS/BS (%)	54.53±3.44*	14.69±3.73	39.84±4.91	55.73±8.83*	15.45±3.98	40.28±7.39
MAR (μm/day)	1.08±0.11*	0.36±0.04	0.73±0.13	1.32±0.20*	0.34±0.05	0.98±0.18
BFR/BS (μm^3/μm^2/yr)	246.78±39.22*	21.31±5.67	225.48±42.59	320.61±79.16*	22.51±8.49	298.10±74.18

MS/BS: mineralizing surface
MAR: mineral appositional rate
BFR/BS: bone formation rate
*: p<0.001, significantly different from the left ulna.

Table 2. Skeleton response to Mechanical Loading in Cav1.3$^{+/+}$ and Cav1.3$^{-/-}$.

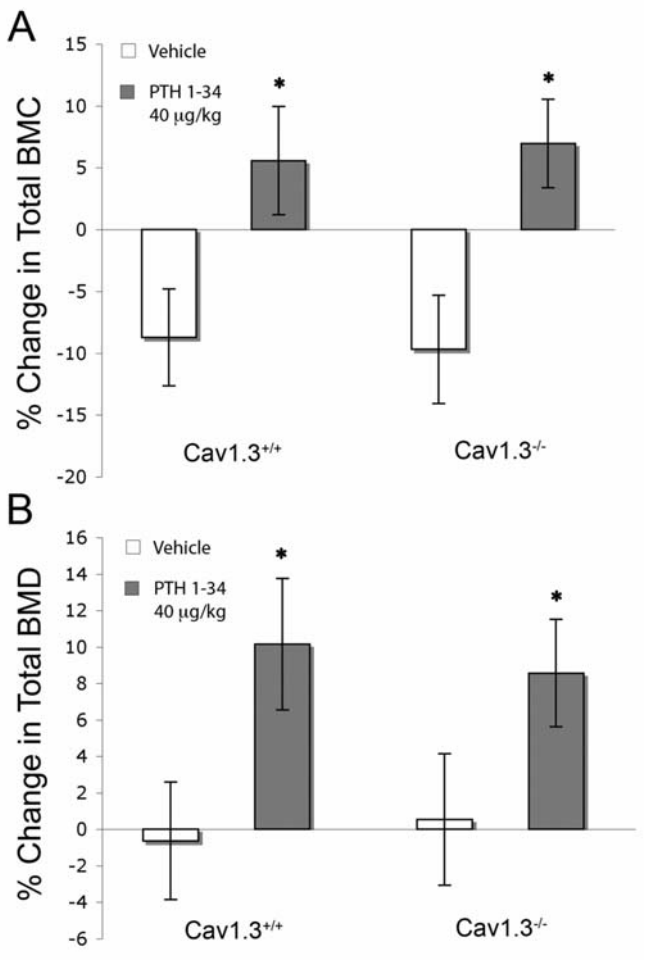

Figure 4. Six weeks of intermittent PTH treatment (40 μg/kg/day) causes similar increases in bone mineral density and content in wild type and Cav1.3 null mice. This graph indicates the changes in bone mineral density (BMC) (**A**) and bone mineral content (BMD) (**B**) before and after PTH treatment measured by *in vivo* pixiMUS scans. BMC showed negative changes and BMD does not change in vehicle treated mice. The percent changes in BMC and BMD compared with vehicle treated mice was not significantly different between wild type control and Cav1.3 null mice. However, BMC and BMD increased markedly in all PTH treated animals. PTH significantly improved BMC and BMD in both wild type and Cav1.3 null mice in comparison with vehicle treated animals. *: $p<0.05$ vs. the vehicle control.

genotype and treatment effect ($p<0.05$), but a significant interaction between genotype and treatment was not detected, suggesting that PTH enhanced hindlimb BMC and BMD significantly and equally in Cav1.3$^{-/-}$ and WT mice.

Histomorphometric measurements in the trabecular bone of the distal femur revealed a slight increase in bone volume between male Cav1.3$^{-/-}$ and WT mice (Table 3). PTH improved mineral appositional rate (MAR) and Bone formation rate (BFR/BS) significantly in both WT and Cav1.3$^{-/-}$ mice (Table 3). Similar to BMC, analysis of variance revealed significant overall genotype and treatment effect ($p<0.05$), but a significant interaction between genotype and treatment was not detected.

To further study the skeletal response to PTH treatment, we dissected out the whole femurs and subjected them to biomechanical testing. With regard to biomechanical properties, Cav1.3$^{-/-}$ mice responded to PTH in the similar manner as WT mice. Under 3-point bending conditions, the femoral shafts from both PTH treated Cav1.3$^{-/-}$ and WT mice were stiffer, and failed at a significantly higher force than the vehicle treated animals (Table 3). The difference between vehicle and PTH treated mice was about 21% in stiffness and ranged from 18 to 27% in ultimate force.

Discussion

This study aimed to understand the role of Cav1.3 in the skeletal response to mechanical loading and intermittent PTH treatment. Cav1.3 null mice demonstrate normal bone development. However, loss of Cav1.3 results in a smaller skeleton in male mice. Mice with a null mutation of Cav1.3 respond normally to mechanical loading and intermittent PTH treatment. Our data suggest that Cav1.3 does not mediate load- and PTH-induced bone formation.

The L-type VSCC messenger RNA for α_1 subunits have been found in primary osteoblasts, stromal precursor cells, osteocytes and osteoblast-like clonal cell lines (for review, see Duncan et al., 1998[8]). Blockade of L-type VSCC using nifedipine has been shown to eliminate the load-induced production of nitric oxide and prostaglandin E_2 in bone organ culture[18]. The critical role of these channels in normal bone physiology has been shown in a study in which nifedipine was given to growing rabbits over 10 weeks[19]. Significant reduction in cancellous and cortical bone volume, mineral apposition and length of the epiphyseal growth plate were observed. In our study, Cav1.3 mRNA is found in osteoblasts. Cav1.3 expression is not detected in Cav1.3 knock-out mice. The null mutation of Cav1.3 led to lower bone mineral content and smaller bone geometry in male mice, suggesting Cav1.3 subunit is important in normal bone growth.

Nifedipine suppressed the cultured osteoblast-like cell's response to oscillatory flow[20] and to the combined effects of fluid shear and PTH[21]. Our previous study has further shown that inhibition of L-type VSCC by verapamil and nifedipine decreases loading induced bone formation *in vivo*[3]. In our present study, Cav1.3 knock-out responded to loading as well as the normal mice. Our data indicated that Cav1.3 does not mediate mechanically induced bone formation. These data suggest that other α_1 subunits may play critical role in mechanotransduction in bone cells.

The results from our PTH experiment, indicating that intermittent PTH treatment was fully anabolic in Cav1.3$^{-/-}$ mice, were surprising. PTH improved bone formation and strength in both Cav1.3$^{+/+}$ and Cav1.3$^{-/-}$ mice. We had anticipated that Cav1.3 inactivation would inhibit the anabolic response to PTH based on a previous report that Cav1.3 can be selectively activated by PTH[10]. Therefore, the combined effects of shear fluid and PTH in osteoblasts, which has been reported previously[21], probably

Parameter	$Cav1.3^{+/+}$		$Cav1.3^{-/-}$	
	Vehicle	PTH	Vehicle	PTH
Animal Number	**n=8**	**n=7**	**n=6**	**n=8**
Body mass (g)	27.86±0.65[c]	31.86±1.34[a,b]	24.47±1.64[c]	26.64±0.72[a]
Distal femur histomorphometry				
BV/TV (%)	10.24±1.61	11.64±1.31	9.32±0.89	12.36±1.64
MS/BS (%)	47.86±2.20	46.30±1.68	44.92±1.84	41.88±3.53
MAR (μm/day)	1.24±0.13	1.97±0.38[c]	1.20±0.09	1.99±0.19[c]
BFR/BS ($\mu m^3/\mu m^2/yr$)	214.58±23.97	329.19±58.64[c]	195.12±15.87	305.20±39.22
Midshaft femur mechanical properties				
Ultimate force (N)	27.06±1.96	32.85±1.98[d]	25.59±1.80	35.23±1.18 b
Stiffness (N/mm)	107.82±9.86	136.94±9.71	111.53±12.78	142.72±9.16
Work to failure (mJ)	7.28±0.61	8.84±1.38	7.38±0.69	7.47±0.54

BV/TV: one volume
MS/BS: mineralizing surface
MAR: mineral appositional rate
BFR/BS: bone formation rate
[a]$p<0.01$, significantly different between genotypes for a given treatment.
[b]$p<0.01$, significantly different from the Vehicle.
[c]$p<0.05$, significantly different between genotypes for a given treatment.
[d]$p<0.05$, significantly different from the Vehicle.

Table 3. Skeleton response to PTH treatment in Male $Cav1.3^{+/+}$ and $Cav1.3^{-/-}$.

mediate via other α_1 subunits, such as Cav1.1 and Cav1.2.

In this study, Cav1.1 and Cav1.2 mRNA levels are found to be up-regulated significantly in $Cav1.3^{-/-}$ mice compared to the normal control. Because null mutation of Cav1.3 does not affect mechanically induced bone formation and PTH anabolic effect in this study, it is possible that enhanced Cav1.1 and Cav1.2 expression compensate the loss of Cav1.3 to maintain the bone anabolic response to loading and PTH. These data suggest Cav1.1 and Cav1.2 may play an important role in mechanotransduction.

We observed sex-dependent differences in the severity of the phenotype in Cav1.3 mutant mice. The Cav1.3 knockout males showed significantly smaller bone size and bone mineral content when compared to the normal males. There is a possibility that Cav1.3 knockout mice may have stopped growing earlier. Unfortunately, we do not have any data on younger animals to verify this possibility. There was no difference between Cav1.3 knockout females and the control. The reason for these disparities between the sexes is still unclear. In our study, we have found that Cav1.3 mRNA level in male wild type mice is significantly higher than female wild type mice. These data suggest a relationship between testosterone and Cav1.3 expression.

In conclusion, Cav1.3 is involved in bone metabolism, especially in male mice. Cav1.3 does not mediate osteoblast response to mechanical loading and PTH. Other α_1 subunits of L-type VSCC, such as Cav1.1 and Cav1.2, may play an important role in mechanotransduction.

Acknowledgement

This study was supported by NASA grant NNA04CD04G (JL) and National Institutes of Health Grant R01DK058246 (RLD) and R01AR046530 (CHT).

References

1 Hung CT, Allen FD, Pollack SR, Brighton CT. Intracellular Ca^{2+} stores and extracellular Ca^{2+} are required in the real-time Ca^{2+} response of bone cells experiencing fluid flow. J Biomech 1996;1411-7.

2 Reid IR, Civitelli R, Halstead LR, Avioli LV, Hruska KA. Parathyroid hormone acutely elevates intracellular calcium in osteoblastlike cells. Am J Physiol 1987; E45-51.

3 Li J, Duncan RL, Burr DB, Turner CH. L-type calcium channels mediate mechanically induced bone formation *in vivo*. J Bone Miner Res 2002;1795-800.

4 Ryder KD, Duncan RL. Parathyroid hormone modulates the response of osteoblast-like cells to mechanical stimulation. Calcif Tissue Int 2000;241-6.

5 Yamaguchi DT, Hahn TJ, Iida-Klein A, Kleeman CR, Muallem S. Parathyroid hormone-activated calcium channels in an osteoblast-like clonal osteosarcoma cell line. cAMP-dependent and cAMP-independent calcium channels. J Biol Chem 1987;7711-8.

6 Chow JW, Fox S, Jagger CJ, Chambers TJ. Role for parathyroid hormone in mechanical responsiveness of rat bone. Am J Physiol 1998;E146-54.

7 Li J, Duncan RL, Burr DB, Gattone VH, Turner CH. Parathyroid hormone enhances mechanically induced bone formation, possibly involving L-type voltage-sensitive calcium channels. Endocrinology 2003;1226-33.
8 Duncan RL, Akanbi KA, Farach-Carson MC. Calcium signals and calcium channels in osteoblastic cells. Semin Nephrol 1998;178-90.
9 Ertel EA, et al. Nomenclature of voltage-gated calcium channels. Neuron 2000;533-5.
10 Barry EL, Gesek FA, Froehner SC, Friedman PA. Multiple calcium channel transcripts in rat osteosarcoma cells: selective activation of alpha 1D isoform by parathyroid hormone. Proc Natl Acad Sci USA 1995;10914-8.
11 Liu R, et al. Ribozyme ablation demonstrates that the cardiac subtype of the voltage-sensitive calcium channel is the molecular transducer of 1, 25-dihydroxyvitamin D(3)-stimulated calcium influx in osteoblastic cells. J Biol Chem 2000;8711-8.
12 Namkung Y, et al. Requirement for the L-type $Ca(^{2+})$ channel alpha(1D) subunit in postnatal pancreatic beta cell generation. J Clin Invest 2001;1015-22.
13 Platzer J, et al. Congenital deafness and sinoatrial node dysfunction in mice lacking class D L-type Ca^{2+} channels. Cell 2000;89-97.
14 Zhang Z, et al. Functional roles of Cav1.3(alpha1D) calcium channels in atria: insights gained from gene-targeted null mutant mice. Circulation 2005;1936-44.
15 Zhang, H. et al. Association of CaV1.3 L-type calcium channels with Shank. J Neurosci 2005; 1037-1049.
16 Schnoke M, Midura RJ. Pulsed electromagnetic fields rapidly modulate intracellular signaling events in osteoblastic cells: comparison to parathyroid hormone and insulin. J Orthop Res 2007;933-40.
17 Torrance AG, Mosley JR, Suswillo RF, Lanyon LE. Noninvasive loading of the rat ulna *in vivo* induces a strain-related modeling response uncomplicated by trauma or periostal pressure. Calcif Tissue Int 1994;241-7.
18 Rawlinson SC, Pitsillides AA, Lanyon LE. Involvement of different ion channels in osteoblasts' and osteocytes' early responses to mechanical strain. Bone 1996;609-14.
19 Duriez J, Flautre B, Blary MC, Hardouin P. Effects of the calcium channel blocker nifedipine on epiphyseal growth plate and bone turnover: a study in rabbit. Calcif Tissue Int 1993;120-4.
20 You J, et al. Osteopontin gene regulation by oscillatory fluid flow via intracellular calcium mobilization and activation of mitogen-activated protein kinase in MC3T3-E1 osteoblasts. J Biol Chem 2001;13365-71.
21 Ryder KD, Duncan RL. Parathyroid hormone enhances fluid shear-induced $[Ca^{2+}]_i$ signaling in osteoblastic cells through activation of mechanosensitive and voltage-sensitive Ca^{2+} channels. J Bone Miner Res 2001;240-8.